

# The Interaction of Iron during the Hot-Pressing of Silicon Nitride

A. D. Stalios, J. Luyten

SCK/CEN, Materials Development Department, Boretang 200, 2400 Mol, Belgium

C. D. Hemsley, F. L. Riley\*

Division of Ceramics, School of Materials, University of Leeds, Leeds LS2 9JT, UK

&

R. J. Fordham

JRC, 1755 ZG Petten, The Netherlands

(Received 9 August 1990; accepted 21 September 1990)

## Abstract

*Microstructural analysis of a commercial hot-pressed silicon nitride containing the equivalents of 1.2 mass % MgO and 2.7 mass % Fe<sub>2</sub>O<sub>3</sub>, shows the existence of intergranular-phase forsterite–fayalite solid solution (olivine), together with iron silicides. The results of modelling hot-pressing experiments carried out at 1500°C with iron(III) oxide and iron additions suggest that the function of iron compounds during hot-pressing is complex, and includes the formation of low-melting transient liquids in the FeO–MgO–SiO<sub>2</sub> system which can be very effective densification aids. Metallic iron appears to yield readily an equally effective iron silicide liquid.*

*Bei der Untersuchung des Gefüges von industriell heißgepreßtem Siliziumnitrid mit einem Anteil von 1.2 Gew.% MgO und 2.7 Gew.% Fe<sub>2</sub>O<sub>3</sub> wurde eine Korngrenzenphase aus Forsterit (Mg<sub>2</sub>SiO<sub>4</sub>)–Fayalit (Fe<sub>2</sub>SiO<sub>4</sub>)–Mischkristallen (Olivin) zusammen mit Eisensiliziden gefunden. Die Auswertung modellhafter Heißpreßexperimente, die bei 1500°C mit Fe(III) Oxid und mit Eisen als Sinterhilfsmittel durchgeführt wurden, lassen vermuten, daß die Wirkungsweise der Eisenverbindungen während des Heißpressens kompliziert ist und die Bildung von die Verdichtung sehr fördernden niedrig schmelzenden und rekristallisierenden flüssigen Phasen im FeO–*

*MgO–SiO<sub>2</sub> System mit einschließt. Die Wirkung metallischen Eisens beruht wahrscheinlich auf der schnellen Bildung einer gleichermaßen wirksamen Eisen-Silizid-Schmelze.*

*L'analyse microstructurale d'un nitrure de silicium pressé à chaud contenant les équivalents de 1.2% massiques de MgO et 2.7% massiques de Fe<sub>2</sub>O<sub>3</sub> a permis de mettre en évidence la présence d'une phase intergranulaire de solution solide forsterite–fayalite (olivine) et de siliciures de fer. Les résultats des expériences de pressage à chaud réalisées à 1500°C avec des ajouts d'oxyde de fer(III) et de fer suggèrent que le rôle des composés ferreux lors du pressage à chaud est complexe et comprend la formation de liquides intermédiaires de bas point de fusion appartenant au système FeO–MgO–SiO<sub>2</sub> qui peuvent être des aides à la densification très actifs. On a également montré que le fer métal peut aisément conduire à une phase liquide de siliciure de fer tout aussi active.*

## 1 Introduction

Many densification additive systems have been investigated for silicon nitride based materials.<sup>1–3</sup> The major requirement is for a liquid-phase forming system which will permit rapid solution and transport of silicon nitride in order to achieve densification, and which will subsequently yield the

\* To whom correspondence should be addressed.

minimum volume of a stable and refractory intergranular phase. Currently used systems are primarily based on MgO, Al<sub>2</sub>O<sub>3</sub> and Y<sub>2</sub>O<sub>3</sub>, although other lanthanide oxides such as Nd<sub>2</sub>O<sub>3</sub> and CeO<sub>2</sub> have also received considerable attention.<sup>4,5</sup> Additions are normally made at the 1–10 mass % level, the larger amounts being needed for pressureless sintering; hot-pressing or hot-isostatic pressing can be accomplished with lesser volumes. Some of the less stable transition metal oxides have been explored for the production of prototype commercial materials. These oxides have included chromium(III) oxide (Cr<sub>2</sub>O<sub>3</sub>) and iron(III) oxide (Fe<sub>2</sub>O<sub>3</sub>), which appear to aid the sintering process, although there seems to have been no detailed exploration of their exact function.<sup>6,7</sup> Iron is also a common impurity in silicon and silicon nitride powders, although the amounts present are normally small. The final state of much of the transition metal is in silicides such as MSi or MSi<sub>2</sub>.<sup>8</sup> The sintering of silicon nitride with magnesium oxide and 2 mass % of iron has been reported,<sup>9,10</sup> where the iron had been introduced during milling of the silicon nitride powder. Early work on the influence of iron oxide additions on the high-temperature properties of hot-pressed silicon nitride shows that at levels up to 0.2 mass % it is without significant effect.<sup>11</sup>

As part of a recent study<sup>12</sup> of the high-temperature corrosion behaviour of a hot-pressed silicon nitride containing magnesium (1.2 mass % equivalent of MgO) and iron (2.7 mass % equivalent of Fe<sub>2</sub>O<sub>3</sub>) densification aids (molar ratio MgO/Fe<sub>2</sub>O<sub>3</sub> = 1.75), detailed microstructural examinations have been made of the starting hot-pressed silicon nitride. On the basis of the information obtained, a supporting investigation has been made into the behaviour of iron oxide and iron in the presence of magnesium oxide during the hot-pressing of silicon nitride, the results of which are reported here.

## 2 Experimental

Surfaces of a commercial silicon nitride disc (Feldmühle, FRG, major densification aids MgO and Fe<sub>2</sub>O<sub>3</sub>; traces of Al<sub>2</sub>O<sub>3</sub> (0.2%), CaO (0.25%), ZrO<sub>2</sub> (0.01%)) were ground to remove approximately 50 µm of possibly contaminated material. Cubes of side 7 mm were cut and polished to 1 µm diamond for SEM and XRD examination. Selected samples of materials were machine thinned to 100 µm, and 3 mm diameter discs were cut and

**Table 1.** Silicon nitride densification additives

Composition	Additive (mass %)				
	MgO	Fe <sub>2</sub> O <sub>3</sub>	Fe	SiO <sub>2</sub>	Y <sub>2</sub> O <sub>3</sub>
A	1.2	0	0	0	0
B	1.2	2.7	0	0	0
C	1.2	0	1.9	0	0
D	1.2	0	0	2.0	0
E	1.2	0	0	0	3.8

dimpled to 5–10 µm for argon ion-beam thinning at an incident angle of 15°. A 20 nm film of carbon was applied to prevent surface charging in a Jeol transmission electron 2000CX microscope equipped with an energy dispersive X-ray analysis (EDX) facility. During examinations particular attention was paid to intergranular-phase material.

Silicon nitride compositions, based on that of the commercial material, were prepared as shown in Table 1; the weights of additives used were chosen on the basis of equivalent molar proportions.

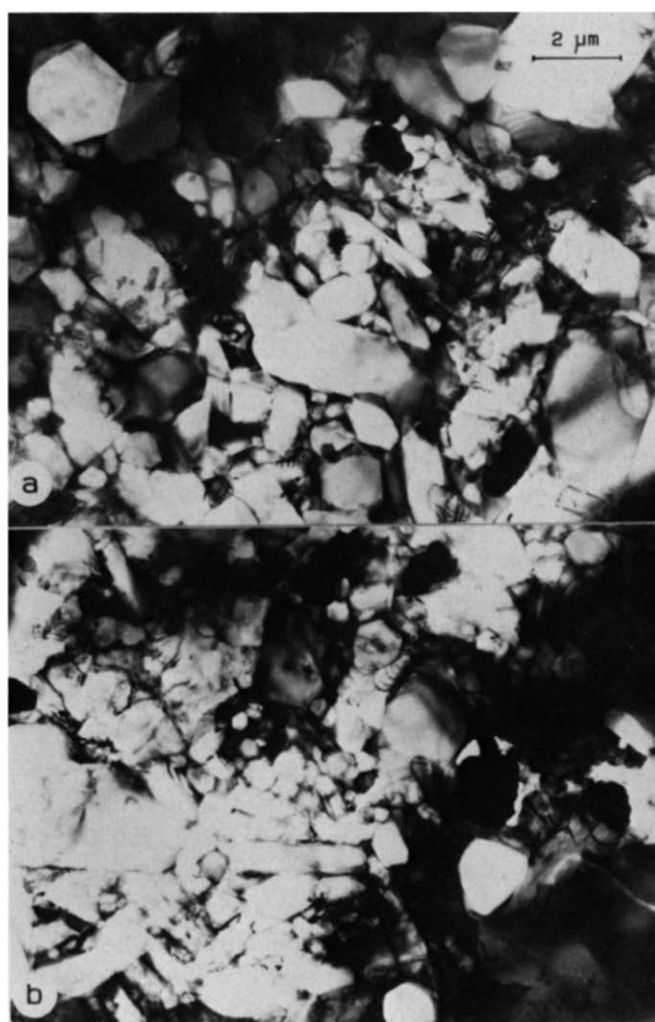


**Fig. 1.** The overall microstructure of two areas of the commercial hot-pressed silicon nitride showing the typical slightly elongated  $\beta$ -Si<sub>3</sub>N<sub>4</sub> grains of hexagonal symmetry.

The silicon nitride powder was Starck LC12 N grade, reported to consist of 95%  $\alpha$ -phase of specific surface area  $22 \text{ m}^2 \text{ g}^{-1}$ , and to have an oxygen content of 1.57 mass % (equivalent to 2.95 mass % of silicon dioxide). The metallic impurity level was negligible. Powder mixtures were obtained by blending solutions of nitrates (magnesium, iron(III) and yttrium), or powders ( $\text{SiO}_2$  and Fe) in propan-2-ol with the silicon nitride powder, followed by drying with constant stirring.

Mixtures were hot-pressed in a boron nitride powder-coated graphite die (25 mm diameter) at  $1500^\circ\text{C}$  and 20 MPa pressure, the nitrates being decomposed *in situ*, on heating.  $1500^\circ\text{C}$  was selected as the densification temperature because it is below the melting point of iron(III) oxide and thus facilitates the detection of processes involving the interaction of iron(III) oxide with other components of the reaction system. In the hot pressing procedure, the pressure (20 MPa) was first applied to the cold powder in the die and then released. The temperature was then raised by  $100^\circ\text{C}/\text{min}$  until the desired value ( $1500^\circ\text{C}$ ) was reached; the pressure was then reapplied ( $t=0$ ). Powder shrinkage was continuously recorded during densification, and after measurement of the final pellet density by water immersion, data were automatically processed to yield plots of density as a function of time, and densification rate as a function of density. Disc

surfaces were polished for SEM and XRD examination.

### 3 Results

Figure 1 is a TEM micrograph of a typical area of the commercial hot-pressed material, which shows the size, distribution and morphology of the  $\beta$ -silicon nitride grains. The mean dimension is of the order of  $1 \mu\text{m}$ , but some grains have long axis dimension as large as  $12 \mu\text{m}$ . Occasionally, at higher magnification,  $\text{Si}_2\text{N}_2\text{O}$  grains are seen with stacking fault sequences parallel to the  $[001]$  direction. Much of the intergranular phase is crystalline. Figure 2, imaged in bright field (BF) and dark field (DF) with the  $0\bar{2}0$  reflection of forsterite,  $\text{Mg}_2\text{SiO}_4$  (ASTM 34-189) shows the extended formation of the phase with this crystal structure. Some of this phase lies along grain faces, and in other regions small  $\beta$ -silicon nitride grains are completely immersed in the phase. Iron is present in the intergranular siliceous phase, as is shown by the EDX pattern of Fig. 3, as traces in partly crystalline material, and in large amounts (Fig. 4) in crystalline material. The iron-containing crystalline phase seen in Fig. 4 has the forsterite structure and therefore corresponds to the forsterite-fayalite solid solution  $(\text{Mg,Fe})_2\text{SiO}_4$ , olivine (ASTM 31-795).

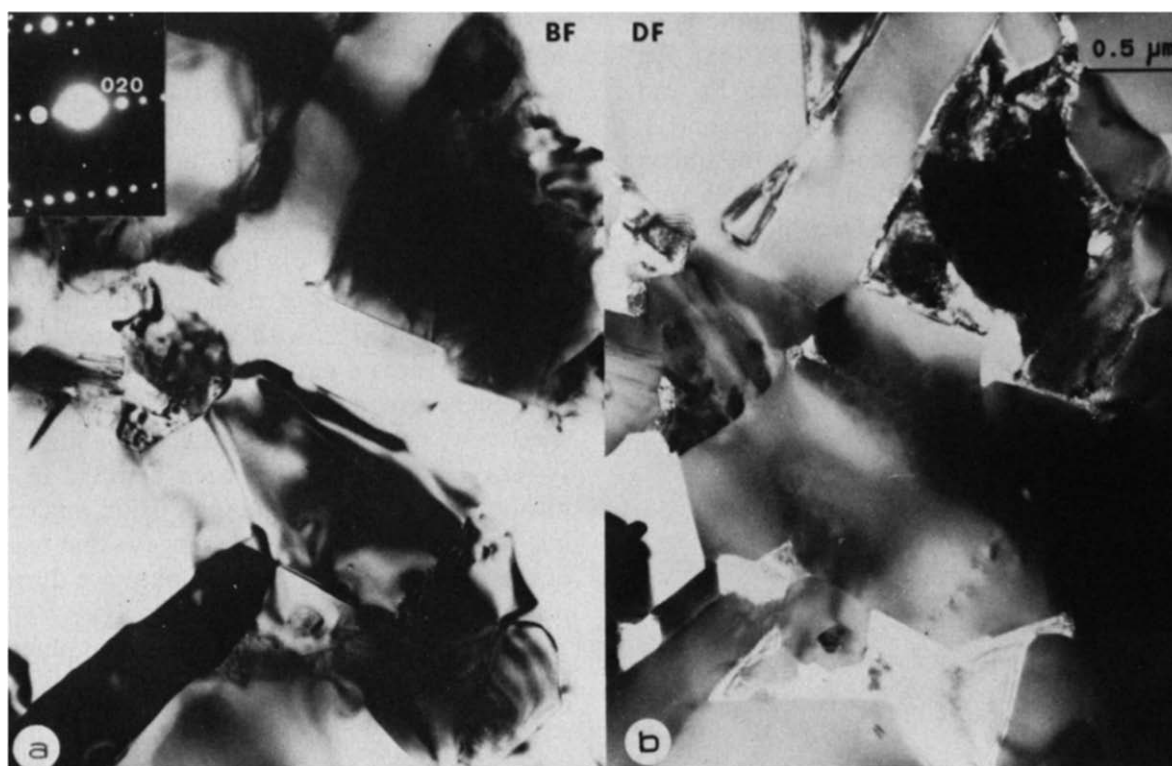


Fig. 2. Intergranular phase material with the forsterite ( $\text{Mg}_2\text{SiO}_4$ ) structure: (a) bright field and (b) dark field imaged with the  $\text{Mg}_2\text{SiO}_4$   $0\bar{2}0$  reflection.

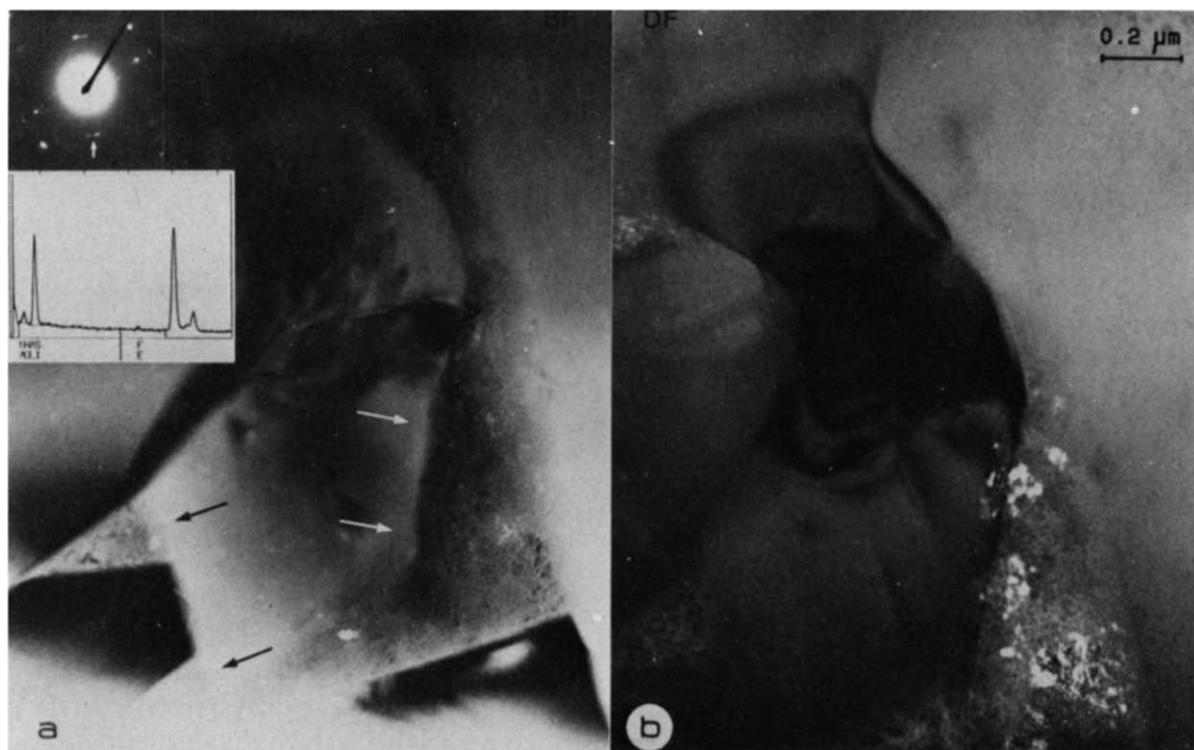


Fig. 3. Partially crystalline, Fe-containing phase (arrowed); (a) bright field and (b) dark field imaged with the  $\text{Mg}_2\text{SiO}_4$  011 diffraction ring (arrowed).

Hot-pressing densification data are shown in Figs 5 and 6. The action of iron(III) oxide in assisting densification is clear. Comparison of the behaviour of compositions B and E shows that iron(III) oxide is as effective an additive under these conditions as yttrium oxide ( $\text{Y}_2\text{O}_3$ ), and more effective than the additional silicon dioxide of composition D, and added to simulate the possible action of iron(III) oxide in generating  $\text{SiO}_2$  by oxidation of the silicon nitride. Metallic iron (composition C) is also a very effective densification aid in the presence of magnesium oxide.

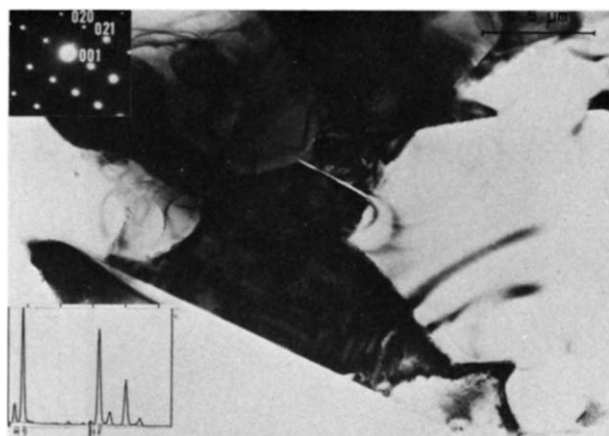
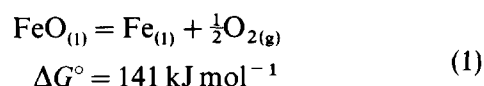


Fig. 4. Crystalline intergranular phase (dark) with the forsterite structure and containing a large proportion of Fe.

#### 4 Discussion

Iron(III) oxide melts at  $1566^\circ\text{C}$  and forms no compounds with  $\text{SiO}_2$ . At  $1500^\circ\text{C}$  in the low oxygen pressure environment of the silicon nitride powder and graphite die, rapid decomposition of the iron(III) oxide to  $\text{Fe(II)O}$  melting at  $1370^\circ\text{C}$  would be expected, with the strong probability that fayalite will be subsequently formed through reaction with surface silicon dioxide. Fayalite melts at  $1205^\circ\text{C}$ , and the adjacent binary eutectics in the  $\text{FeO-SiO}_2$  system are  $1178$  and  $1177^\circ\text{C}$ .<sup>13</sup> These temperatures are considerably lower than that of the enstatite peritectic at  $1557^\circ\text{C}$  with which forsterite can co-exist. There are no ternary compounds in the  $\text{MgO-FeO-SiO}_2$  system and so the appearance of liquid is effectively determined by the  $\text{FeO-SiO}_2$  binary system. Fayalite has also been detected in silicon nitride sintered with magnesium oxide, and containing iron as impurity.<sup>9,10</sup> This suggests that oxidation of the iron to iron(III) oxide took place during wet processing.

$\text{FeO}$  itself has an equilibrium oxygen potential at  $1550^\circ\text{C}$  of  $5 \times 10^{-9}$  bar for  $a_{\text{FeO}} = 1$ :



A second important function of the transition

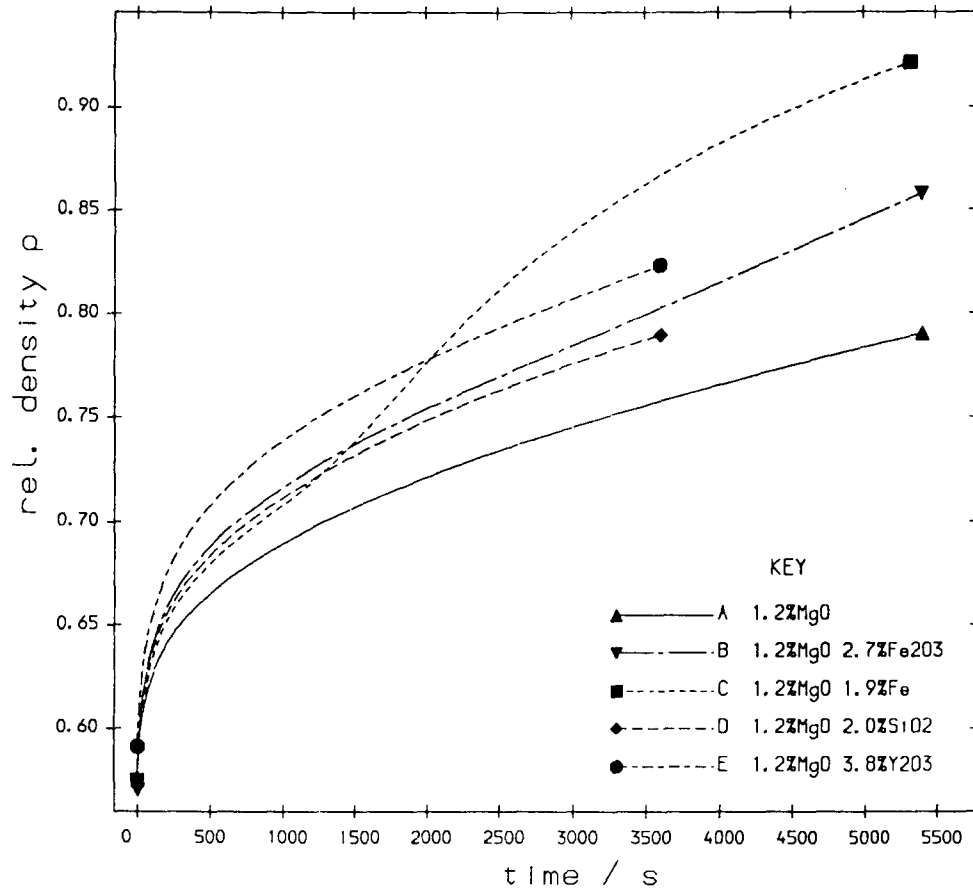


Fig. 5. Density as a function of time at 1500°C for compositions A to E under 20 MPa pressure.

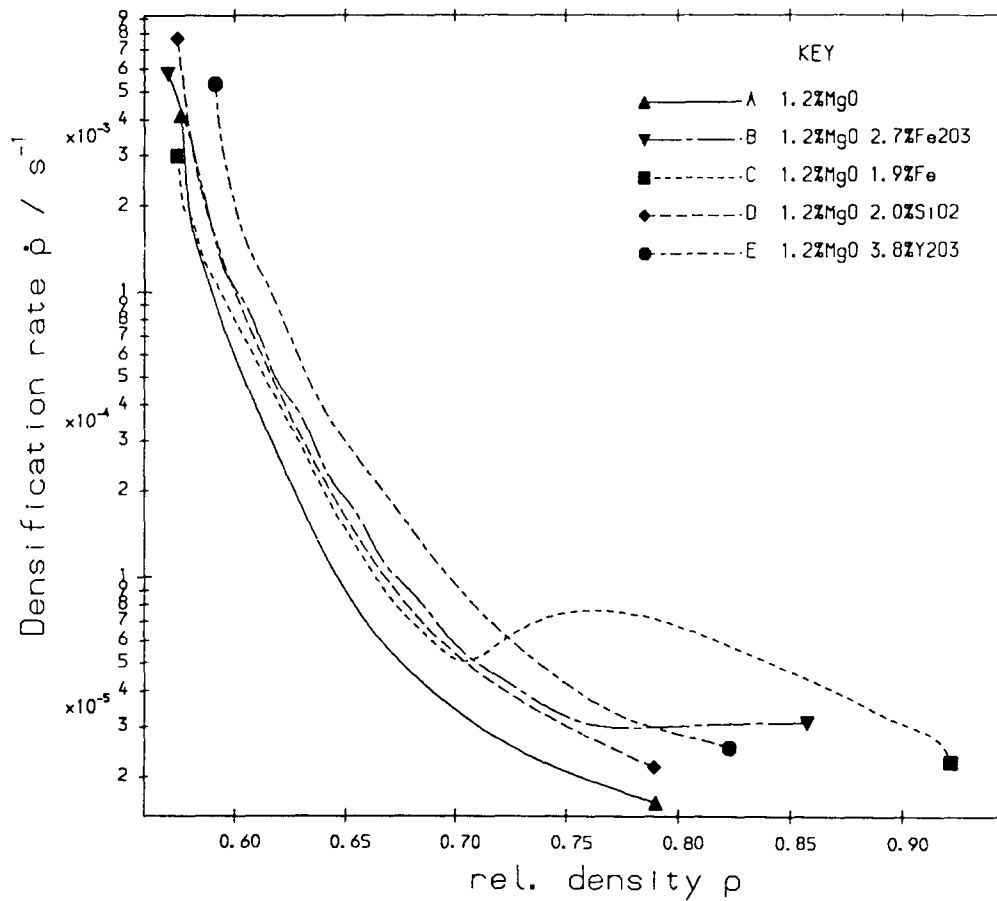


Fig. 6. Densification rate as a function of density; data derived from those shown in Fig. 5.

metal oxide is thus to provide a source of oxygen, which by reaction with silicon nitride will form an equivalent quantity of silicon dioxide:



In the case of silicon nitride powders of low natural oxygen content this silicon dioxide could be beneficial in generating a larger volume of liquid silicate. With the  $\text{MgO-Fe}_2\text{O}_3$  systems used here the intergranular phase composition will be moved away from forsterite towards enstatite, and an increase in the volume of 'enstatite liquid' would occur. The influence of varying  $\text{MgO/SiO}_2$  ratios on the properties of hot-pressed silicon nitride has been examined in some detail.<sup>15</sup> The transition metal is able to react further, however. Because iron nitride,  $\text{Fe}_4\text{N}$ , is unstable under 1 bar  $\text{N}_2$  at temperatures  $>25^\circ\text{C}$ , fast reaction of the iron released by reduction of the oxides to form silicides would be expected:



$\text{FeSi}$  melts at  $1410^\circ\text{C}$ , and liquid is present for compositions richer in silicon at temperatures above  $\sim 1210^\circ\text{C}$ .<sup>8</sup> The apparent lack of wetting of the silicon nitride by silicide, or the lower surface energy of the silicon nitride-silicate interface, leads to the appearance of isolated liquid globules ultimately yielding particulate inclusions in the intergranular regions of the silicon nitride. The silicide thus provides an effective trap for the transition metal as is demonstrated on subsequent high-temperature oxidation, where although ready outwards diffusion of silicate metal cations ( $\text{Mg}$  and  $\text{Y}$  for example) can occur to generate oxide film silicates, very little migration of the silicide metallic element can be detected.<sup>16</sup>

The function of the iron(III) oxide in this system is complex: it provides a transient liquid silicate in the fayalite system, additional silicon dioxide, and finally liquid silicides. It thus becomes difficult to predict the precise effects on densification rate.

The most significant feature of the microstructure of the commercial material is the forsterite-fayalite (olivine) solid solution detected in the intergranular phase material. Most of the iron is present as the silicides  $\text{FeSi}$  and  $\text{FeSi}_2$  which is its anticipated final state, considering the instability of the iron oxides in the reducing atmosphere of the graphite hot-pressing die, and the presence of the silicon nitride.

$\text{Fe(II)O}$  would be expected to be temporarily stabilised through olivine formation giving  $a_{\text{FeO}} \ll 1$  and a corresponding decrease in the oxygen equilibrium pressure. Consistent with the above discussion,

the microstructural analysis makes it clear that  $\text{Fe(II)O}$  has been formed at an intermediate stage of the reduction process, traces of which remain in the intergranular olivine at completion of the hot-pressing. The tendency for iron to be located in the crystalline rather than the amorphous intergranular silicate suggests that the forsterite-structure phase crystallises more readily when  $\text{Fe}^{2+}$  is present.

The action of iron(III) oxide in assisting densification is shown clearly in the data presented in Figs 5 and 6. By comparison with reference composition A containing only magnesium oxide, composition B densifies very rapidly and at higher temperatures full density would be expected to be readily attained. Comparison between compositions B and E shows that iron(III) oxide is slightly more effective, on a molar basis, than  $\text{Y}_2\text{O}_3$ . A significant feature of the iron(III) oxide densification curve is the period of acceleration after 2 ks. This is most likely due to the appearance at this point of liquid iron silicide. Metallic iron (composition C) shows behaviour similar to iron(III) oxide in the later stages of densification but with more marked acceleration after 1 ks, to provide confirmation of this action. This indicates appreciable solubility of silicon nitride in  $\text{FeSi}_x$  liquids, and would suggest that the final isolated state of the silicide is the result of a lower nitride-silicate interfacial energy. The development of  $\beta\text{-Si}_3\text{N}_4$  from iron-rich regions during the nitridation of silicon powder<sup>17</sup> shows that nitrogen has appreciable solubility in  $\text{FeSi}_x$ ; dissociation and solution of  $\text{Si}_3\text{N}_4$  is also a possibility therefore. The use of additional silicon dioxide (composition D) gives some acceleration of densification, but the relative weakness of this effect makes it clear that the most important function of the iron(III) oxide in the initial stages of densification is that of providing the transient liquid  $\text{Fe(II)}$  silicate.

## 5 Conclusions

The use of a reducible transition metal oxide such as iron(III) oxide in conjunction with other, thermodynamically more stable, oxides can be of benefit in the densification of silicon nitride through the formation of transient binary and ternary liquid silicates, as well as by providing an in-situ source of silicon dioxide. Continuing reduction of the oxide leads ultimately to the formation of low-melting silicides. It seems that the most important of these effects in the case of iron(III) oxide additions are those of the formation of low-melting compositions in the  $\text{FeO-MgO-SiO}_2$  system, and finally liquid

iron silicide ( $\text{FeSi}_x$ ). Iron impurities in silicon nitride powder thus tend to act as additional and very effective densification aids.

### Acknowledgements

This work has been partly supported by the Commission of the European Communities through Stimulation Action Contract ST2J-0146-UK(CD) and through EURAM programme MA1E-0037-C(A). Dr E. Gilbert provided assistance with hot-pressing facilities.

### References

1. Terwilliger, G. R. & Lange, F. F., Pressureless sintering of  $\text{Si}_3\text{N}_4$ . *J. Mat. Sci.*, **10** (1975) 1169–74.
2. Lange, F. F., Silicon nitride polyphase systems: Fabrication, microstructure and properties. *Int. Metals Rev.*, **1** (1980) 1–20.
3. Jack, K. H., The significance of structure and phase equilibria in the development of silicon nitride and sialon ceramics. In *Science of Ceramics*, Vol. 11, ed. R. Carlsson & S. Karlsson. Swedish Ceramic Society, 1981, pp. 125–42.
4. Weaver, G. Q. & Lucek, J. W., Optimisation of hot-pressed silicon  $\text{Si}_3\text{N}_4$ - $\text{Y}_2\text{O}_3$  materials. *Am. Ceram. Soc. Bull.*, **57**(12) (1978) 1131–6.
5. Pomeroy, M. J., Saruhan, B. & Hampshire, S., Kinetics of densification and transformation in silicon nitride sintered with mixed neodymia/magnesia additions. In *Special Ceramics 8, Proc. Brit. Ceram. Soc.*, Vol. 37, ed. S. P. Howlett & D. Taylor. The British Ceramic Society, Stoke-on-Trent, 1986, pp. 21–8.
6. Godfrey, D. J., Fabrication, formulation, mechanical properties and oxidation of sintered  $\text{Si}_3\text{N}_4$  using disc specimens. *Mat. Sci. Tech.*, **1** (1985) 510–15.
7. Cotton, J. W. & Swindells, R., European Patent Application 0 107 919, 9 May 1984.
8. Hansen, M. & Andoko, K. (eds), *Constitution of Binary Alloys*, 2nd ed. McGraw-Hill, New York, 1958.
9. Giachello, A. & Popper, P., Sintering of silicon nitride at atmospheric pressure. In *Ceramics for High Performance Applications III*, ed. E. M. Lenoe, R. N. Katz & J. J. Burke. Plenum Press, New York, 1983, pp. 347–57.
10. Popper, P., Sintering of silicon nitride: A review. In *Progress in Nitrogen Ceramics*, ed. F. L. Riley. Martinus Nijhoff, 1983, pp. 187–210.
11. Iskoe, J. L., Lange, F. F. & Diaz, E. S., Effect of selected impurities on the high-temperature mechanical properties of hot-pressed silicon nitride. *J. Mater. Sci.*, **11** (1976) 908–12.
12. Stalios, A. D. & Luyten, J., Transmission electron microscopy characterisation of an MgO-containing hot-pressed silicon nitride. Progress Report S-10/1989, CEC Contract No. ST2J-0146-3-B.
13. Robbins, C. R. & McMurdie, H. F., *Phase Diagrams for Ceramists*. The American Ceramic Society, Columbus, Ohio, Fourth Printing, 1979.
14. Elliott, J. F. & Gleiser, M., *Thermochemistry for Steel-making*. Addison-Wesley, Reading, MA, 1960.
15. Lange, F. F., Phase relations in the system  $\text{Si}_3\text{N}_4$ - $\text{SiO}_2$ -MgO and their interrelation with strength and oxidation. *J. Amer. Ceram. Soc.*, **61** (1–2) (1978) 53–6.
16. Andrews, P. & Riley, F. L., The microstructure and composition of oxide films formed during high-temperature oxidation of a sintered silicon nitride. *J. Eur. Ceram. Soc.*, **5**(4) (1989) 245–56.
17. Campos-Loriz, D. & Riley, F. L., Factors affecting the formation of the  $\alpha$ - and  $\beta$ -phases of silicon nitride. *J. Mat. Sci.*, **13** (1978) 1125–7.